

# EVS BASED APPROACH PROCEDURES: IR-IMAGE ANALYSIS AND IMAGE FUSION TO SUPPORT PILOTS IN LOW VISIBILITY

Hans-Ullrich Doehler, Bernd Korn

Institute of Flight Guidance, German Aerospace Research Center, DLR, Braunschweig, Germany

**Keywords:** *Enhanced vision, image analysis, data fusion*

## Abstract

Based on a recently released new flight rule by the Federal Aviation Administration (FAA) a dream of imaging technology enthusiasts becomes reality:

*Visual guidance (VFR) of landing aircraft in adverse weather is no longer restricted by the performance of the human eye (measured as runway visual range, RVR). Based on the output of imaging sensors it is now allowed to continue the approach beyond the classical minimum decision altitude (MDA) or decision height (DH) down to about 100 ft whenever at DH or MDA the runway can be clearly identified within the sensor image.*

*This rule change in aircraft operation will allow to conduct bad weather landings to non-ILS- equipped airfields and without an expensive on-board ILS installation.*

*However, after this “quantum leap in flight rule making” new questions are coming up: “How to inform the pilot what the imaging sensor just sees?” Usually, a (quite expensive) Head Up Display (HUD) is required to show the output of the sensed image, which is presented in a raster scan overlay onto the existing stroke vector image. Is this “direct overlay method”, which “blocks” the transparency of the HUD, really the best way to do this, or are there other options to make-up enhanced visual aircraft guidance concepts and systems?*

*The following contribution tries to give some hints for answering these questions and proposes a more transparent EVS display format. A new method for extracting the aircraft*

*position relative to the runway in real-time from the on-board imaging sources is presented.*

*Finally, some experimental results from flight trials during the US-American SE-Vision project, where the described method has been implemented and tested, are explained.*

## 1 Introduction

Enhanced Vision Systems (EVS) are aiming to alleviate restrictions in airspace and airport capacity in low visibility conditions. EVS relies on weather-penetrating forward-looking sensors that augment the naturally existing visual cues in the environment and provide a real-time image of prominent topographical objects that may be identified by the pilot. The basic idea behind this technology is to allow VMC operations under IMC. The recently released final rule of the FAA [1] for Enhanced Flight Vision Systems (EFVS) for part 92 aircraft (business aircraft, general aviation aircraft) clearly acknowledges the operational benefits of such a technology by stating the following: “Use of an EFVS with a HUD may improve the level of safety by improving position awareness, providing visual cues to maintain a stabilized approach, and minimizing missed approach situations“ (Federal Aviation Administration, 2004, p. 1621). Moreover, “The pilot would use this enhanced flight visibility ... to continue the approach from DH [decision height] or MDA [minimum descent altitude] down to 100 ft above the touchdown zone elevation of the runway of intended landing” (p. 1621). This rule change marks a significant token of confidence

towards EVS technology and clearly demonstrates that EVS offers the capability to decrease landing minima and thus, increase accessibility of airports (even of non-equipped airports) under low visibility conditions. Furthermore, they offer the possibility for reduction of radar separation in case the pilot is able to clearly detect the leading aircraft in the sensor image. One mayor advantage of EVS is that it can be easily used in combination with other landing aids like e.g. SBAS. Allowing the pilot to “see” under low visibility conditions, EVS increases safety and offers the possibility to increase accessibility and capacity by reducing landing minima or even by reducing separation distances.

## 2 Enhanced Vision Systems – Principles of Operation

It easily can be seen that the performance of the Enhanced Vision System is strongly depending of the selection of imaging sensors. At DH (or MDA) of the flown approach procedure the pilot has to use EVS as primary input to continue the approach down to the new EVS DH after which visual contact to the runway has to be established. Infra-red (IR) and millimeter-

display (HUD). However, the penetration of bad weather (dense fog and light rain) in the infrared spectrum is remarkably poorer than the weather penetration that can be achieved by MMW-radar. An active MMW-radar delivers primarily information about the range and the angular direction (azimuth) of a certain object. This range/angle information can be transformed into a view “out-of-the-window”, but there is still a lack of information about the objects’ height or their vertical position. The presentation of such images needs knowledge about the surrounding elevation, which often is estimated by the so-called “flat-earth-assumption”.

### 2.1 The SE-Vision Project

An important topic for integrating new visual sensors into existing cockpit environments concerns the question on how to visualize the acquired images and/or visual cues. An obvious method for showing this information is a simple overlay onto the head-up-display (HUD) as transparent raster image. Due to its simplicity this method has been applied in several enhanced vision projects in the past [2]-[10]. In the US American SE-Vision program, which was finished with several demonstration flights



Fig. 1. SE-Vision Project. a) FAA’s Test Aircraft Boeing 727 on Atlantic City Airport, b) Max-Viz IR-Camera System, c) Installed Flight Test Equipment.

wave (MMW) sensors are currently envisaged as the most promising EVS support of pilot vision in low visibility. One important benefit of IR-sensors is that these sensors generate a perspective image, from which the human can derive the perceptual cues of depth to generate a three-dimensional interpretation of the outside world. This is an important feature of the IR-sensor as such a perspective sensor image can be overlaid to the outside scene on a head-up

display (HUD). However, the penetration of bad weather (dense fog and light rain) in the infrared spectrum is remarkably poorer than the weather penetration that can be achieved by MMW-radar. An active MMW-radar delivers primarily information about the range and the angular direction (azimuth) of a certain object. This range/angle information can be transformed into a view “out-of-the-window”, but there is still a lack of information about the objects’ height or their vertical position. The presentation of such images needs knowledge about the surrounding elevation, which often is estimated by the so-called “flat-earth-assumption”.

on a Boeing 727 in 2005 (Fig. 1.), a transparent inset method has been investigated, too. Beside several project partners, such as the FAA, Rockwell-Collins and Max-Viz, the German Aerospace Center (DLR) had participated. The objective of the DLR contribution was to demonstrate a more intelligent way of overlaying the information from two different IR-cameras, to reduce cluttering of the HUD and to provide a much better “look through”, so

that pilots can recognize clearly the outside-world shortly before the finally touchdown.

**2.2 Bi-FLIR Camera**

Especially in case of several different imaging sensors, a fusion of the information content from the images has to be carried out in advance. In the SE-Vision project Max-Viz had provided a bi-FLIR camera [11] (Fig. 1. b)), consisting of a long wave IR sensor (LWIR - wavelength 8-13 micron) and a short wave IR-sensor (SWIR - wavelength 1-3 micron). The LWIR “sees” the thermal contrast between the concrete of the runway and the surrounding grass area, and the SIWR image captures runway lamps at the runway border and some other visual navigation aids like VASI or PAPI systems at the left or right side of the runway.

**3 DLR’s Image Processing Scheme**

For both image sources, a separate analysis process extracts hypothesis on the location of the runway structure in each image. This extraction process itself is driven by some structure grouping algorithm based on image features, such as contour lines, contour blobs and so on. For each detected runway structure a

hypothesis on the aircraft position relative to the runway is computed. This computation requires some knowledge about runway data, such as the width and length of the runway stripe, and some camera parameters, like the field of view (FOV) and the coarse orientation of the camera axis relative to the aircraft. Thereafter a fusion process, which is carried in parallel to the image analysis processes, combines these hypotheses from the different image sources over time and space, so that finally, after two or three seconds of consistent data, a valid relative aircraft position relative to the runway is available. This data fusion method has been implemented based on a fuzzy C-Means clustering algorithm, which takes into account that the movement of the aircraft relative to the runway from image to image can be computed easily from the aircraft’s inertial reference system (IRS) data and the known heading of the runway.

**3.1 Relative Position to Runway**

The task of computing the relative geometric position and orientation of a camera, with respect to some well-known objects in 3-D space using images from that camera can be regarded as a solved problem. The applied mathematical toolkit combines elements of linear algebra, such as vector and matrix

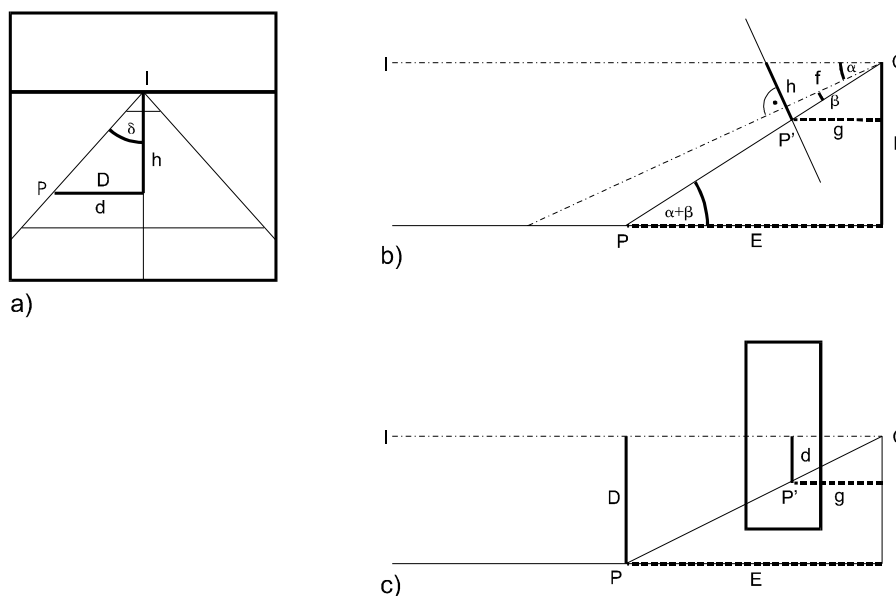


Fig. 2. Perspective projection of the runway stripe: a) image plane, b) side view, c) top view.

multiplication, and some methods for solving a set of equations (i.e. least mean square error). In addition, there is a huge amount of published methods for special applications in this field. But all these methods and algorithms require the knowledge of a minimum set of 3-D points in the scene, their corresponding 2-D coordinates in the image plane, and the parameters of the camera (focal length, size and principal point of the image), as well [11]. Together with a well-calibrated camera, a minimum of three 3-D to 2-D point references are required to compute all six external camera parameters (3 Euler angles and 3 coordinates in 3-D space).

There are published systems for the estimation of an aircraft's position and orientation relative to a runway based on the knowledge of the coordinates of four corner points of the runway stripe and the identification of these points in the image plane, as well [13], [14]. But it is a big disadvantage, that there is a need for some special markings on the runway.

If the exact mounting angles of the camera relative to the aircraft are known, then the camera orientation can be measured by the aircraft's inertial navigation system (INS). In this case, only two point references are required, but the estimation of the aircraft's position relative to the runway is highly affected by camera calibration errors and INS angle errors as well.

To overcome the need of a well calibrated camera and the need for the precise knowledge of some runway reference point locations, the following method has been developed. Some simple geometric

considerations on the image of a parallel structure with respect to the relative position of the imaging camera result in a simple equation to compute the camera position.

Fig. 2 a) shows the perspective image of a runway. The rectangular border of the runway stripe is projected as a trapezoid on the image plane. The right and left border line of the runway intersect at the vanishing point  $I$  on the horizon line. The detailed geometry is shown in Fig. 2 b) as side view and in Fig. 2 c) as top view. It is assumed that the camera is located at the centre of projection  $C$  exactly above the centre line of the runway in a height  $H$  above the runway plane. It is further assumed, that the camera lens has a focal length  $f$  and its optical axis is inclined downwardly by a pitch angle  $\alpha$ . An arbitrary given point  $P$  on the left runway border is assumed to have a lateral distance  $D$  from the centre line and a horizontal distance  $E$  from  $C$  in the runway plane. The image of point  $P$  on the image plane is denoted as  $P'$ , where  $d$  denotes the horizontal, and  $h$  the vertical distance from the vanishing point  $I$ . From the side view in Fig. 2 b) it can be stated that

$$\frac{H}{E} = \tan(\alpha + \beta),$$

and

$$h = f(\tan \alpha + \tan \beta),$$

and finally

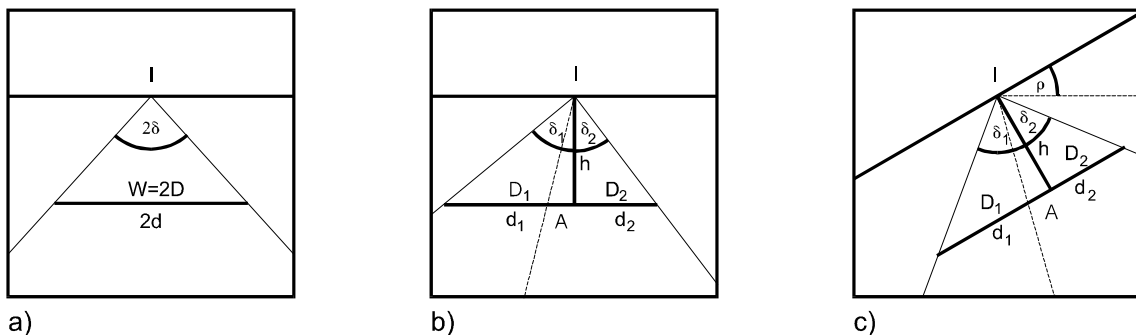


Fig. 3. Perspective projection of the runway stripe: a) above the centre line of the runway, b) lateral offset to the centre line of the runway, c) a rotated camera rotates the image around the vanishing point  $I$ .

$$g = f \frac{1}{\cos \beta} \cos(\alpha + \beta).$$

From the top view in Fig. 1 c) it can be seen that

$$\frac{D}{E} = \frac{d}{g}.$$

It follows that

$$\frac{d}{h} = \frac{D}{H} \frac{\tan(\alpha + \beta) \cos(\alpha + \beta)}{(\tan \alpha + \tan \beta) \cos \beta},$$

which is equal to

$$\frac{d}{h} = \frac{D}{H} \frac{\sin \alpha \cos \beta + \cos \alpha \sin \beta}{\tan \alpha \cos \beta + \sin \beta}.$$

It can be seen that the focal length  $f$  cancels out. The further assumption, that the pitch angle  $\alpha$  is small, which means the camera's optical axis is roughly parallel to the runway stripe, thus  $\sin(\alpha) \approx \alpha$ ,  $\tan(\alpha) \approx \alpha$ , and  $\cos(\alpha) \approx 1$ , leads to

$$\frac{d}{h} = \frac{D}{H} \frac{\alpha \cos \beta + \sin \beta}{\alpha \cos \beta + \sin \beta},$$

and therefore

$$\frac{d}{h} = \frac{D}{H}.$$

Together with the angle  $\delta$ , which is measured in the runway image (Fig. 2 a)), it can be noted

$$\frac{d}{h} = \tan \delta,$$

and it follows the height  $H$  as

$$H = \frac{D}{\tan \delta}.$$

In case of a runway with a known width of  $W=2D$  and for a centered camera (Fig. 3 a)) it follows

$$H = \frac{W/2}{\tan \delta}. \quad (1)$$

For a camera position with a lateral offset  $A$  from the center line, two angles  $\delta_1$  and  $\delta_2$  (Fig. 3 b)) are measured separately and the height above the runway results from the equation

$$H = \frac{W}{\tan \delta_1 + \tan \delta_2}. \quad (2)$$

Finally the lateral offset  $A$  follows from

$$A = \frac{W}{2} - H \tan \delta_2. \quad (3)$$

Regarding practical applications it must be ensured that the camera rotation around the optical axis relative to the runway plane (roll angle  $\rho$ ) is either small or can be measured (see Fig. 3 c)). In principle, there are two methods:

1. identification of a horizontal structure in the image (e.g. the horizon or the base line of the runway) and measurement of the orientation of this structure relative to the horizontal edges of the image, or
2. usage of an external sensor to measure  $\rho$  (e.g. inertial attitude sensor).

As it can be seen from Fig. 3 c), all relations for estimating the height and horizontal offset remain true and can be applied after an inverse

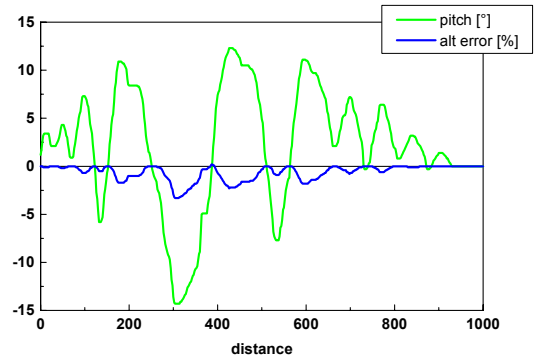


Fig. 4. Simulation results. The altitude error remains below 3% for neglected pitch angles below  $\pm 10^\circ$ .

rotation of the image around point  $I$ .

The above described method for position estimation based on un-calibrated camera images has been filed for patent in 2003, which has been granted in Jan. 2005 [15].

Accuracy considerations based on simulations showed that the introduced error in vertical position due to un-modeled pitch angles between  $\pm 10^\circ$  stays below 3% (Fig. 4), which is better than the accuracy requirements stated by the ICAO for calibration of instrument landing systems (ILS, CAT III), where the glide-path-angle has to be adjusted and maintained within a tolerance of 4% of the nominal glide-path-angle [16].

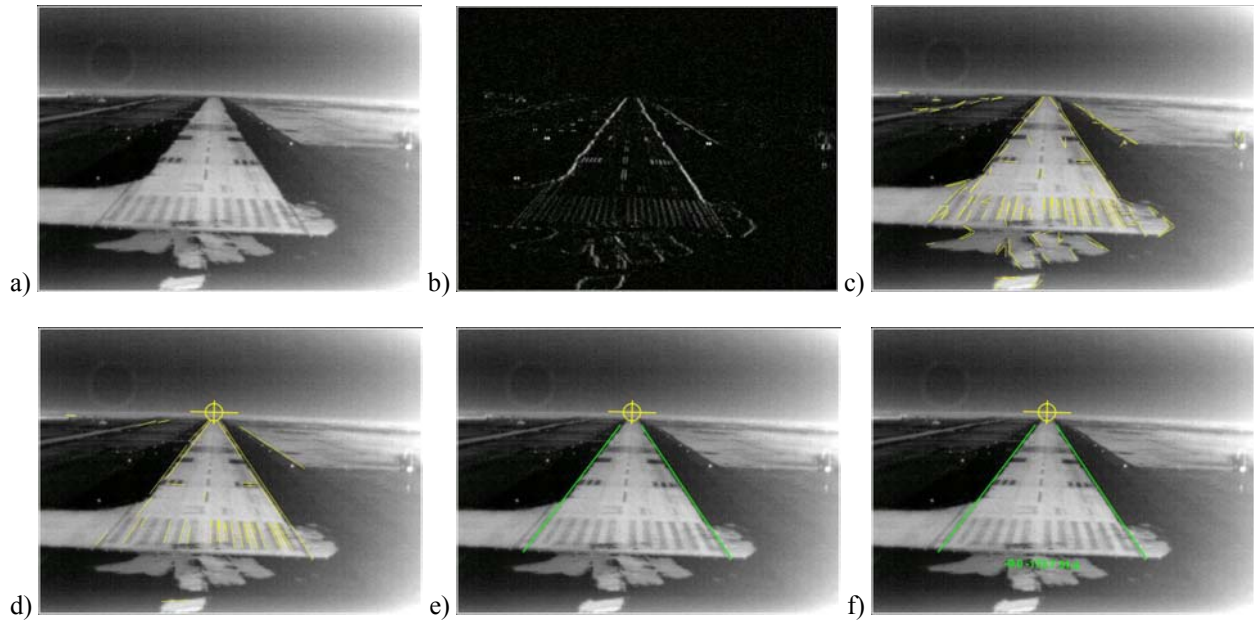


Fig. 5. Processing steps for long wave infrared (LWIR) a) input image, b) horizontal gradient image, c) extracted lines, d) filtered lines, vanishing point marked at the horizon, e) extracted runway border, f) computed relative aircraft position in meter ( $x = 0.0$ ,  $y = -173.7$ ,  $z = 31.4$ )

### 3.2 Image Processing and Image Fusion

Processing and fusion of the incoming long wave and short wave infrared image streams (LWIR and SWIR) applies a image processing chain, which consist of several single steps of image analysis procedures for feature extraction and data fusion. The parameters of each step of this processing chain can be configured and adapted easily (without any recompilation), so that an optimal setting can be achieved after some “fine-tuning” during runtime with respect to the incoming data. For the objective of program stability and re-usability the same process (named “ir\_analysis”) is running on the same computer in two different instances, one for each image stream. A third loosely coupled process (named “ir\_fusion”) is responsible for bringing the results of both image streams together, and delivers its results finally to a fourth process, which controls the other processes and generates the display for aircraft guidance, which can be shown either to the pilot on the HUD or (e.g. for the co-pilot) on a head-down display, as well. All data

communication between these four processes is realized by using a shared memory concept.

Of course, some steps in this processing chain for the long wave infrared images (LWIR, which shows mainly the contrast between grass and concrete, Fig. 5 a)) differ from steps for the short wave infrared images (SWIR, which shows the runway and PAPI lamps, Fig. 6 a)). Without going to much into the details, the processing chain comprises the following steps for each incoming image:

1. LWIR image: Application of some gradient filter algorithms for extracting the runway border line (see Fig. 5 b).
2. LWIR and SWIR image: Converting the gray scale image into a set of binary images (black and white image). This is done by applying a set of binarisation thresholds. Pixels with grey values below the threshold become black; all other pixels become white. Usually, three or four levels of binarisation are sufficient to deal with a “normal” image dynamic.
3. LWIR and SWIR image: Contour extraction and contour following for each generated binary image. The result is a set

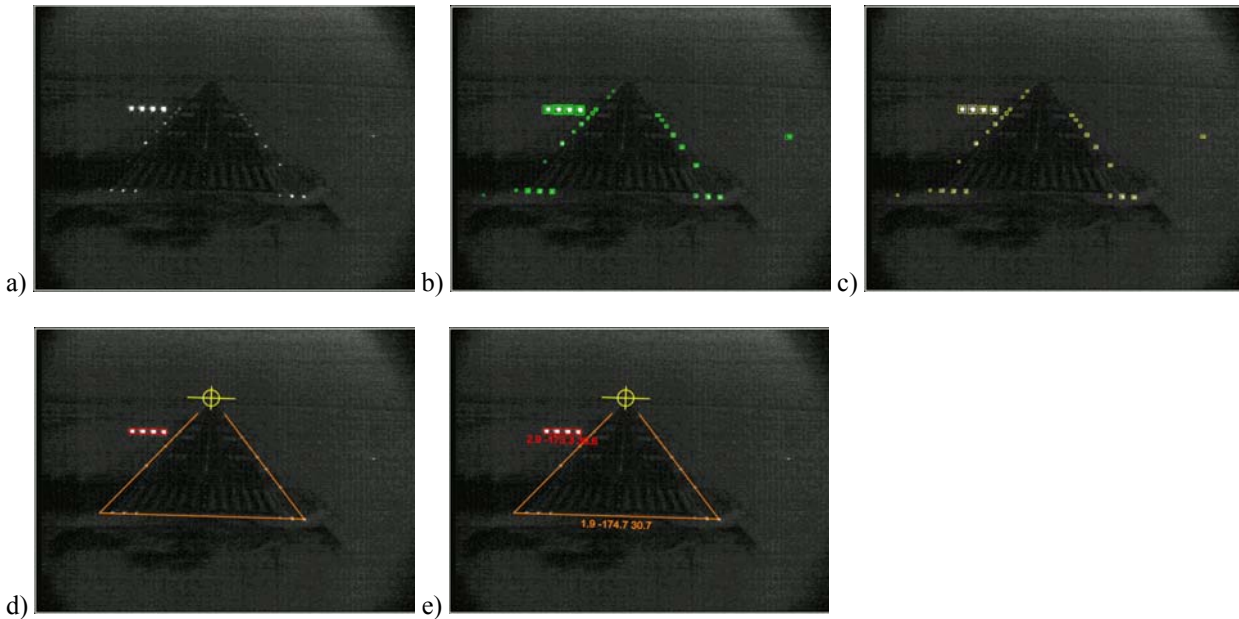


Fig. 6. Processing steps for short wave infrared (SWIR) a) input image, b) detected blobs, d) fused blobs, e) extracted runway border and PAPI lights, vanishing point from INS at the horizon, e) computed relative aircraft position in meter (from runway border:  $x = 1.9, y = 174.7, z = 30.7$ , from PAPI lights:  $x = 2.9, y = 173.3, z = 30.6$ ). These numbers match quite good the results from Fig. 5.

of closed contours, designated by a starting point and a contour-points chain (Freeman-coded).

4. LWIR image: Segmentation of the extracted contour chains into a list of line segments by an orthogonal line regression algorithm (see Fig 5. c) and d)). SWIR images: Extraction of blobs and clustering of single blobs into “blob-lines” (see Fig. 6. b) and c)).
5. Clustering of detected lines into groups

which built up trapezoidal structures; each of them is a so-called “runway-hypothesis”. The estimated location of the vanishing point, which is computed from the INS angles, can be used to reduce the number of possible runway hypotheses. In case of “blob-lines” additional runway hypotheses are generated from possible detected horizontal “blob lines”, which may show (if in the field of view) the PAPI structure on the left or right side of

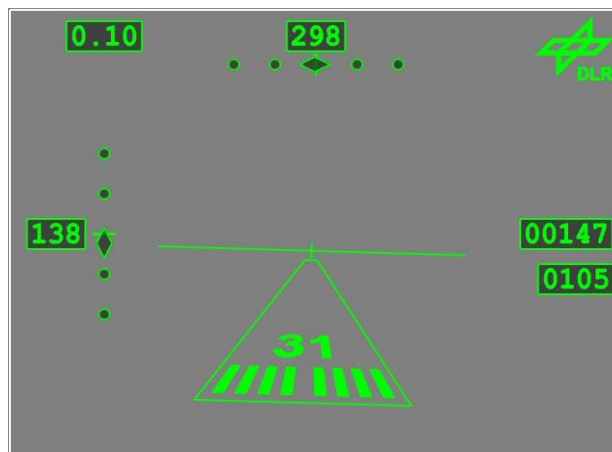


Fig. 7. Display of fusion results. The numbers have the following meaning: **138** : true airspeed in knots, **0.10** : distance to threshold in nautical miles, **298** : true heading in degree, **00147** : barometric altitude in feet, **0105** : computed altitude above threshold in feet. Synthetic runway display in the center (Runway 31) and a virtual ILS glide-slope indication is shown right of speed display and the ILS localizer indication below heading.

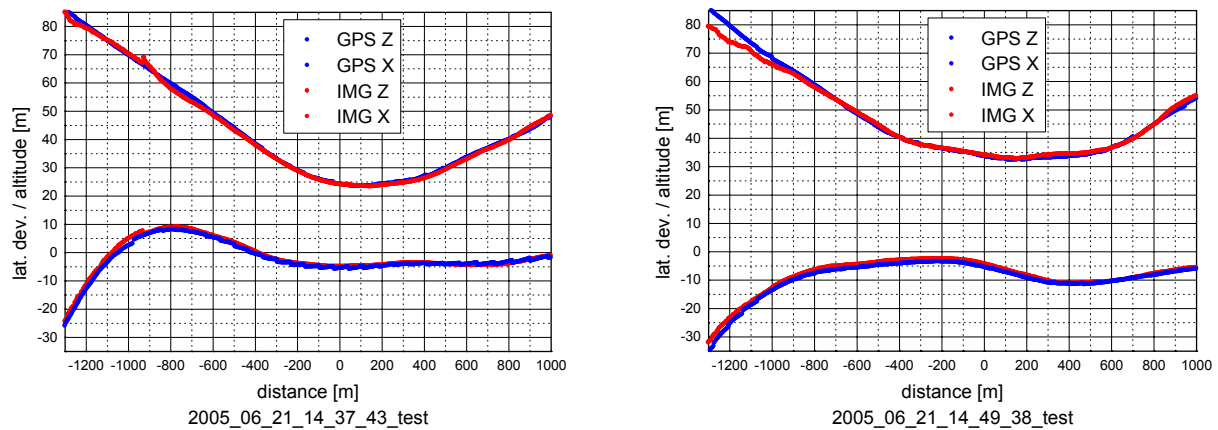


Fig 8. Accuracy of position computation from two different landing approaches (over flights) to runway 28 on Cape May County Airport. The upper part shows the vertical and the lower part the horizontal projection of the aircraft track. The origin of the plots depicts the runway threshold. Blue lines show the D-GPS reference data and red lines the image based aircraft position. Below a distance of about 800 m the error lies in the region of about or even less one meter. For a more detailed analysis of this small error, it would be necessary to get much more accurate data for both, airport reference and D-GPS reference data, as well, which are not available up to now.

- the runway.
6. Estimating the vertical and lateral deviation from the runway left and right border using the above proposed method (Chapter 3.1). The output of this fusion process is a list of possible runway hypotheses, each with certain detection quality and a relative aircraft position.
7. Clustering of the results from LWIR and SWIR image analysis by using a Fuzzy-C-Means clustering algorithm. Each cluster carries data about its quality and has to be shifted from frame to frame by the relative aircraft movement (controlled by INS-NAV data). Usually, after more than 30 frames (i.e. approx. 1 sec.) of consistent incoming image data a clearly best-valued result is extracted, which finally is transferred to the display process.
8. Computing a full transparent “stroke-like” display format for showing the analysis and fusion results to the pilot (see. Fig. 7)

### 3.3 Interpretation of Flight Test Results

The above described DLR’s software packet has been installed into the FAA Boeing 727 test aircraft in January 2005. Flight tests have been conducted from January 2005 until end of June 2005. In principle, the DLR software has been

shown its expected performance, although there had been several minor problems, which could be solved by installing some software updates during the flight test period. Beside its real-time analysis capability, the DLR software has been used for data recording, as well. During these flight tests an amount of about 10 GByte of data together with quite accurate flight test data (such as D-GSPS and INS and others) could be recorded. These data consist of 30 approaches to 6 different runways on four different locations (Alamosa, Atlantic City, Albuquerque and Cape May). With respect to further developments in this field, the value of these data cannot be overestimated.

To get an impression about the accuracy of the extracted aircraft position (in runway coordinates), the recorded D-GPS navigation data is used as basis. Together with runway reference data (e.g. the location of the runway threshold) from these data the relative aircraft position has been computed and can be compared to the image analysis results. Fig. 8 shows two examples. As can be seen, accuracy lies in the region of about one meter, or – in other words – in the same region as the accuracy of the reference data (D-GPS data and airport

reference data, as well). In general, it can be stated, that such accuracy is better than required.

#### 4 Summary and Conclusion

The “native” method of displaying sensed imagery data directly onto a HUD via a simple (pixel-based) inset or overlay concept contains several disadvantages:

- The major advantage (transparency!) of the HUD is vanished by cluttering the display.
- It cannot simultaneously show images from different sources.
- It is normally difficult to interpret.

Our proposed “more intelligent” method of automatically analyzing the (several) incoming image data stream(s), and the extraction of relevant content (the runway), allows overcoming the disadvantages above mentioned:

- The fusion of the analysis results from several imaging sensors and the integrity check against available NAV data delivers one single navigation solution.
- A high transparent display of a perspective symbolic runway is generated from this navigation solution.
- The symbology is easy to interpret.
- Additional aircraft guidance cues can be displayed, such as a virtual ILS-localizer and ILS-glide-slope.

The patented proposed robust method for computing the aircraft position relative to the runway stripe does not require any complex calibration procedure of the applied cameras and sensors, which can be regarded as great advantage. This eases especially system certification and maintenance. The achieved accuracy (less than one meter) of the proposed method over-complies with the requirements.

Compared to infrared cameras, millimeter wave (MMW) radar sensors allow a much better

penetration of the atmosphere, especially in bad weather situations. The next extension of enhanced vision systems will be the integration of these sensors. Compared to IR images, MMW sensor data are much more difficult to interpret and require usually some additional input data (e.g. radar altitude relative to the runway plane). Our proposed concept of automatic image analysis and data fusion will become even more attractive for such enhanced vision system extensions, because no “native” method for displaying MMW radar images directly exists.

#### References

- [1] FAA. Enhanced Flight Vision Systems – Final Rule. Department of Transportation, FAA, 14 CFR Parts 1, 91, 121, 125 and 153, *Federal Register Vol. 69, No. 6, January 9, 2004*, pp. 1619-1641.
- [2] Hecker, P. and Doehler, H.-U. Enhanced Vision Systems: Results of Simulation–and Operational Tests, in Verly, J.G. (Ed.): *Enhanced and Synthetic Vision 1998*, SPIE Vol. 3364.
- [3] Hecker, P., Doehler, H.-U and Suikat, R. Enhanced Vision Meets Pilot Assistance, in Verly, J.G. (Ed.): *Enhanced and Synthetic Vision 1999*, SPIE Vol. 3691.
- [4] Korn, B., Doehler, H.-U. and Hecker, P. Navigation Integrity Monitoring and Obstacle Detection for Enhanced Vision Systems, in Verly, J.G. (Ed.): *Enhanced and Synthetic Vision 2001*, SPIE Vol. 4363.
- [5] Korn, B. and Hecker, P. Enhanced and Synthetic Vision: Increasing Pilot's Situation Awareness under Adverse Weather Conditions. Air Traffic Management for Commercial and Military Systems, *Proceedings of the 21st Digital Avionics Systems Conference, DASC 2002*, Omnipress.
- [6] Korn, B. and Hecker, P. Pilot Assistance Systems: Enhanced and Synthetic Vision for Automatic Situation Assessment. *Proceedings of the International Conference on Human-Computer Interaction in Aeronautics, HCI-Aero 2002*, HCI-Aero, AAAI Press.
- [7] Pirkl, M. and Tospann, F.-J. The HiVision MM-Wave Radar for Enhanced Vision Systems in Civil and Military Transport Aircraft, in Verly, J.G. (Ed.): *Enhanced and Synthetic Vision 1997*, SPIE Vol. 3088, pp. 8-18.
- [8] Beier, K., Fries, J., Müller, R. and Palubinskas, G. IR-measurement and image processing for enhanced vision in civil aviation, in J.G. Verly (Ed.): *Enhanced and Synthetic Vision 2001*, SPIE Vol. 4363.

- [9] Beier, K. and Gemperlein, H. Simulation of infrared detection range at foc conditions for Enhanced Vision Systems in civil aviation, *Aerospace Science and Technology*, Vol 8, 2004, pp.63-71.
- [10] Way S., Kerr R. et.al. Development and testing of the EVS-2000 Enhanced Vision System, in Verly, J.G. (Ed.): *Enhanced and Synthetic Vision 2003*, SPIE Vol. 5081, pp. 51-57
- [11] Max-Viz. <http://www.max-viz.com/product/evs2000.html>, EVS-2500 Specification, Max-Viz, Inc., Portland, OR, USA.
- [12] Fischler, M.A. and Bolles, R.C. Random sample consensus: A paradigm for model fitting with applications to image analysis and automated cartography, *Communications of the ACM*, Volume 24, Number 6.
- [13] Hingst, U. Landeverfahren für unbemannte Flugzeuge, *German Patent*, DE 19521600A1.
- [14] Tarleton, N.G. Method and apparatus for navigating an aircraft from an image of the runway, *United States Patent*, US 6157876.
- [15] Doehler, H.-U. and Korn B. Vermessungsverfahren zur Flug- und Fahrzeugführung, *German Patent*, filed Jan 2003, granted Jan 2005, DE 10305993.
- [16] ICAO. International Standards, Recommended Practices and Procedures for Air Navigation Services, Aeronautical Telecommunications, *Annex 10 to the Convention on International Civil Aviation*, Fourth Edition of Volume I.

## Acknowledgements

This work was sponsored by the German Ministry of Defense entitled “ESVS zur Pilotenunterstützung”.

Thanks to Dick Kerr and Greg Zuro from Max-Viz for providing the computer hardware and camera interface for the DLR’s image processing and runway extraction software.

Thanks to Richard Rademaker from Rockwell-Collins for his excellent support regarding the interface to real-time flight test data. He provided the hard- and software to pump INS and NAV data into DLR’s software and he was responsible for conducting so many flight trials as flight test engineer including the collection of a huge amount of image and flight test data.